THERMAL GENERATING UNIT TRANSIENTS FOLLOWING STEP-CHANGES OF FREQUENCY ("FREQUENCY STEPS")

By
O. P. Geszti—L. Z. Rácz—L. Kiss—I. Horváth and J. Somló
Institute of Heavy Current Engineering, Technical University Budapest

(Received December 8, 1972)

1. Introduction

There is a regular electric energy exchange between Hungary and Austria within the scope of an import-export contract. In the course of this exchange, in summer Austria supplies energy to Hungary, in winter the direction of the energy transfer is the opposite.

The quantity of the imported and exported power is not large in comparison to the installed capacity of the systems: it is generally about 100 MW. For the transmission of this power it was sufficient to set up a transmission line of a single system on 220 kV between Vienna and Győr. In the course of the realization of the energy exchange it was to be taken into consideration that Hungarian energy system is a part of the eastern European co-operation system (CDU) while the Austrian is that of the western one (UCPTE). The installed capacities of both of the systems are so large (that of the CDU system is about 50 and that of the UCPTE is about 100 GW), that it is impossible to establish a parallel operation through a 220 kV line. In account of this, the energy exchange was carried out so, that in the summer period a consumer isle work is performed in the western part of the Hungarian network being supplied by Austria, on the other hand, in the winter period one or two of the turbo-generator blocks of the Oroszlány power plant, separated from the Hungarian system, furnish energy to Austria through the Vienna—Győr and the Győr—Oroszlány lines in co-operation with the Austrian system. The energy export toward Austria is realized always at night in terms of the contract, so the above mentioned blocks in the daytime work in co-operation with the Hungarian system and in the evening they are switched over to the Austrian system as a result of a series of switching operations controlled by a so-called "pseudo-synchronous automation" and initiated by the personnel. In the course of the switching operations, first a circuit breaker joins the Hungarian and the Austrian networks for a short time (0.1 sec) through a prepared current path, thereafter the immediate switching out of an other circuit breaker will again separate the systems so that the corresponding full loaded block or blocks will stay switched on the Austrian network. Since there is often a frequency difference in the order of magnitude of 0.1 Hz, from the point of view of the

generators in question, this phenomenon can be represented by the sudden change of the frequency of the transfer impedance and of the load angle depending on the moment of the switching operation.

For clearing up the transient phenomena following the switching operation and for the determination of the mechanical and thermal stresses, field test measurements followed by analog computer simulations were carried out.

In the present paper the results of the field test measurements and the results obtained by computer simulation as well will be described in detail. The basic equations and the block diagrams of the analog simulation are given in Appendix as well as the legend and the basic data of the computer analysis.

In the following the program of the investigations by analog simulation will be described. Thereafter, the processes at the individual pseudo-synchronous switchings and the effect of the parameters on the magnitude of the electric, mechanic and thermal stresses will be analysed, partly on the basis of the field test measurements, and partly on the basis of the results of analog computer simulations.

A series of registrations obtained by measurements and the corresponding analog computer simulation results are given in the paper. The principal points at the pseudo-synchronous switching are the following:

The transients following the moment of the switching are fundamentally influenced by the instantaneous value of three parameters:

1. the *transfer impedance* between the terminals of the machine and the fictitious infinite bus-bar substituting the network;

2. the *angle difference* of the synchronization (the angle difference of the voltages of the infinite bus-bars substituting the two systems, at the moment of the switching);

3. the *frequency difference* between the systems.

The physical basis of the effect of these parameters is the following:

ad 1. The electric power given by the synchronous generator working parallel in a given network is essentially influenced by the transfer impedance between the generator terminals and the fictitious infinite bus-bar substituting the network. The abrupt change of this impedance occurring for example at a switching operation causes an electric power jump of the machine. In the present case, there is a significant difference between the transfer impedances of the parallel work with the Hungarian and with the Austrian network. So, in the course of a switching, there is a jump in the electric power.

ad 2. The second parameter influencing the power supplied into the network by a synchronous machine is the load angle.

In the course of the pseudo-synchronous switching the instantaneous relative angle position of the systems is determined by the moment of the switching, on the other hand, there are different load angles belonging to the

same power in the two systems, so the instantaneous angle difference may cause a jump in the electric power of the machine at the switching.

ad 3. Since before the switching the speed of rotation of the synchronous machine is determined by the frequency of the network and the frequency after the switching may differ from it, so after switching, in the electric power of the machine an asynchronous component will appear, depending on the magnitude of the frequency difference.

Each of the factors mentioned above may have three essentially different values from the point of view of the switching:

1. The transfer impedance may increase, decrease, or stay unchanged.
2. The change of the load angle may be positive, negative or zero.
3. At last, the frequency difference may also be positive, negative or practically zero.

In this way, in principle, there are 27 possible cases for these three parameters. This situation becomes more complicated because of the influence of the regulators (quick excitation regulator, turbine regulator) and of the reactive power supplied at the moment of switching.

The phenomenon is considered energetically so that the synchronous machine must take up or give off kinetic energy, depending on the sign of the frequency step. In the case of the increase of the kinetic energy, for example, the energy surplus is partly supplied from the electric side. The value of the energy, taken from the electric side is evidently influenced by the value of the switching angle difference and by the change of the transfer impedance.

2. The evaluation of the effect of the important parameters on the process of the pseudo-synchronous switching

In the following the role of the different factors influencing essentially the switching processes will be outlined on the basis of the summarized results of computer simulation and of the field test measurements.

2.1. The effect of the electric power of the steady-state preceding the switching

The difference between the nominal power and the power before the switching influences, primarily, the non-electric quantities.

In evaluating the results of the measurements it was stated that in the 50 MW working point the change of the mechanical power of the turbine, caused by the switching, would remain below 2 MW, provided that the frequency step was less than 0.7 Hz. This is negligible from the point of view of the process. The maximum of the pressure difference percentage between the nominal and the measured values is given in Table 1. This occurred at a fre-

Table I

Working point power	P (MW)	50	30
The change of the regulating oil pressure in comparison to its working point value	$\frac{100\ \Delta p_s}{p_{sm}}$ (%)	3.6	29.3
The pressure change of the center wheel in comparison to its working point value	$\frac{100\ \Delta p_c}{p_{cm}}$ (%)	1.3	15.4
The pressure change of the 5th tap in comparison to its working point value	$\frac{100\ \Delta p_5}{p_{5m}}$ (%)	1.0	8.5
The pressure change of the 3rd tap in comparison to its working point value	$\frac{100\ \Delta p_3}{p_{3m}}$ (%)	0	5.8
The axial displacement in comparison to the maximum value occurring at the tearing	$\frac{100\ \Delta x}{0.6}$ (%)	3.2	100

quency step of 0.39 Hz, the maximum in course of the measurements. Table 1 contains also the maximum values of the relative axial displacement caused by the values of the pressure changes given in Table 1 as well. In simulation, at the 30 MW working point, the change of the mechanical power given off by the turbine was reckoned with (in conformity with the results of the field tests measurements). It is to be mentioned, however, that this power change does not influence essentially the electric parameters of the switching.

The switching at a working point different from the nominal is disadvantageous because the increase of the axial displacement cannot be calculated previously and so no controllable value can be reached.

The axial displacements at the switchings in the case of different loads are time functions and cannot be determined because the change of the pressure of the individual taps can only be identified by the analog model at the working points where measurements were carried out.

2.2. The influence of the frequency step (Δf)

The influence of the frequency difference between the systems (Δf) could not be evaluated from the field test measurements since its value was between 0.3 and 0.39 in all of the measured cases. In the course of the computer simulation it was possible to vary the value of Δf over a sufficiently wide range: beyond the frequency step of the field test measurements (which proved to be of middle size among the cases occurring in practice). The value 0.7 Hz, the limit according to the present prescriptions, was also studied. At last, the Δf value causing just a switch in the shaft-coupling torque was search-

ed for and an analog simulation was carried out for this case too (in the two latter cases the switching angle was at its optimum value — see 2.3. for further explanation).

The conclusions are the following:

In the case of positive frequency steps (frequency increase at the Δf of the measurements 0.35 Hz in average), the amplitude of the first — negative — electric power peak was 60% of the nominal power for high and 56% for low reactive power supplies; the following positive maximum values of the power were in both cases 145%. At the limit value of Δf (0.7 Hz, being approximatly the double of the previous value) the first negative peak was 150% and 120%, respectively; the first positive maximum value was 188% and 196%, respectively. The frequency step belonging to the limit power of the shaft coupling moment change is 0.88 Hz for low, and 0.83 Hz for high reactive power; namely in average it is only 20% higher than the limit according to the present prescriptions.

For negative frequency steps the mechanical stresses were higher than for positive ones, since the electrical relation with the network was much stricter in this case and so the synchronizing moments were also much higher. It should be added that according to the analog computer studies, the requirement of the stability limits less the allowed value of the limit frequency step. This is proved also by the fact that in the case of $\Delta f = 2$ Hz the transient stability will safely be maintained but such a high frequency difference cannot be allowed from the point of view of the mechanical stresses.

2.3. The influence of the switching angle difference ($\Delta\delta$)

The value of the angle difference between the voltages of the two systems at the moment of the switching can be considered as a random variable. On the basis of the measurements carried out, and of theoretical causes, it can be supposed to have a normal distribution since it is a linear function of the total operating time of the circuit breakers and the control blocks (for constant Δf). (In the following the type of the $\Delta\delta$ distribution will be irrelevant.)

If the angle difference between the voltage vectors of the systems is zero at the moment of switching, then there is a precise synchronization. Since the switching of the machine is carried out under load and the values of the transfer impedance until the infinite bus-bar are different before and after switching, so a non-zero value of $\Delta\delta$ is necessary for a switching without power step (this is the so-called "smooth" switching). This is the value of $\Delta\delta_{opt}$, which does not depend upon Δf. If in a switching $\Delta\delta \neq \Delta\delta_{opt}$, then an electric power step will appear. In the course of the field test measurements because of the inadequate possibilities of adjustment — among the 18 measurements only in a single case happened an approximately smooth switching. The effec-

tive $\Delta\delta$ values were to be determined from the analog simulation for the measured cases (see the analog computer and field test registrations as well given in diagrams 1 to 14).

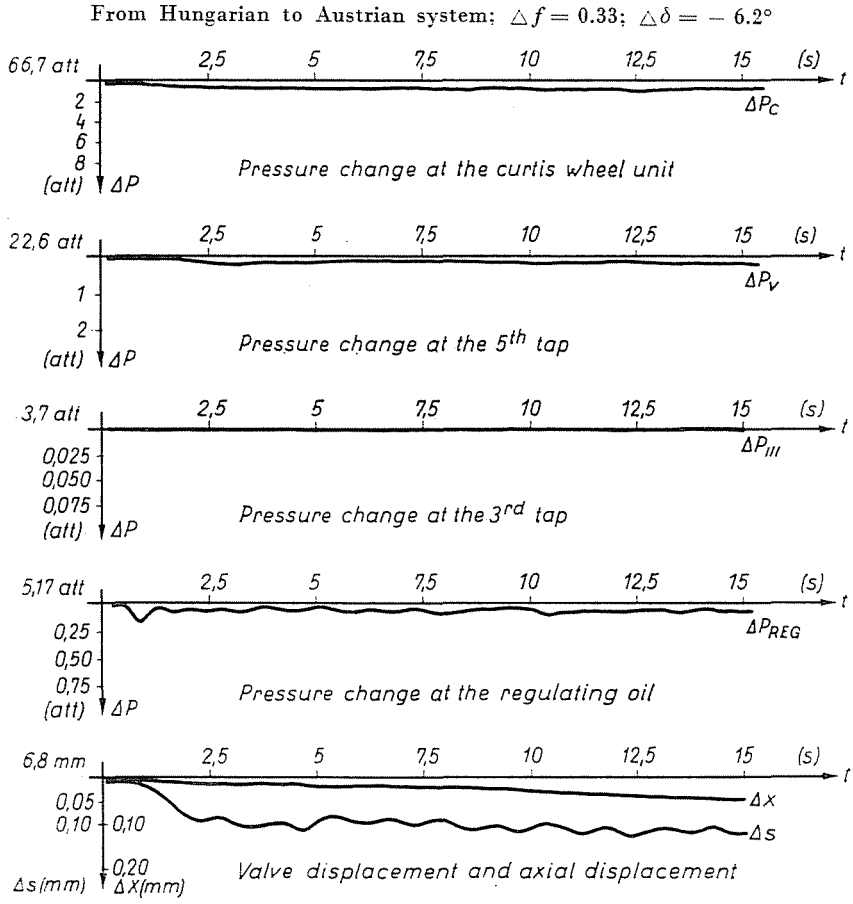

MEASURED VALUES

Diagram 1

The experiences of the analog computer analysis concerning the influence of $\Delta\delta$ are the following:

a) In the case of positive frequency step, for a high reactive power (35 MVAr) $\Delta\delta_{opt} = 11.3°$, for a low reactive power (10 MVAr) $\Delta\delta_{opt} = 11.8°$; for a simultaneous switching of two machines and 120 kV transmission voltage level: $\Delta\delta_{opt} = 20.5°$, and in the case where the transmission line worked on 220 kV: $\Delta\delta_{opt} = 16.1°$. It was examined also that for $\Delta f = 0.7$ Hz, which are the values of $\Delta\delta_{max}$ and $\Delta\delta_{min}$ that will cause just a shaft-coupling torque switch.

It resulted that the interval without shaft-coupling torque switch was approximately symmetrical on $\Delta\delta_{opt}$; the values of $\Delta\delta_{max} - \Delta\delta_{opt} \cong \Delta\delta_{opt} - \Delta\delta_{min}$ averaged in the case of high reactive power 18°, and for low reactive power 21.5°.

b) In the case of negative frequency step, the value of $\Delta\delta_{opt}$ averages —8°, when a single machine is switched; in the case of two machines with a transmission line working on 120 kV, it is —17.2°, and with that of 220 kV it is —12.5° according to the analog computer studies. The results of these

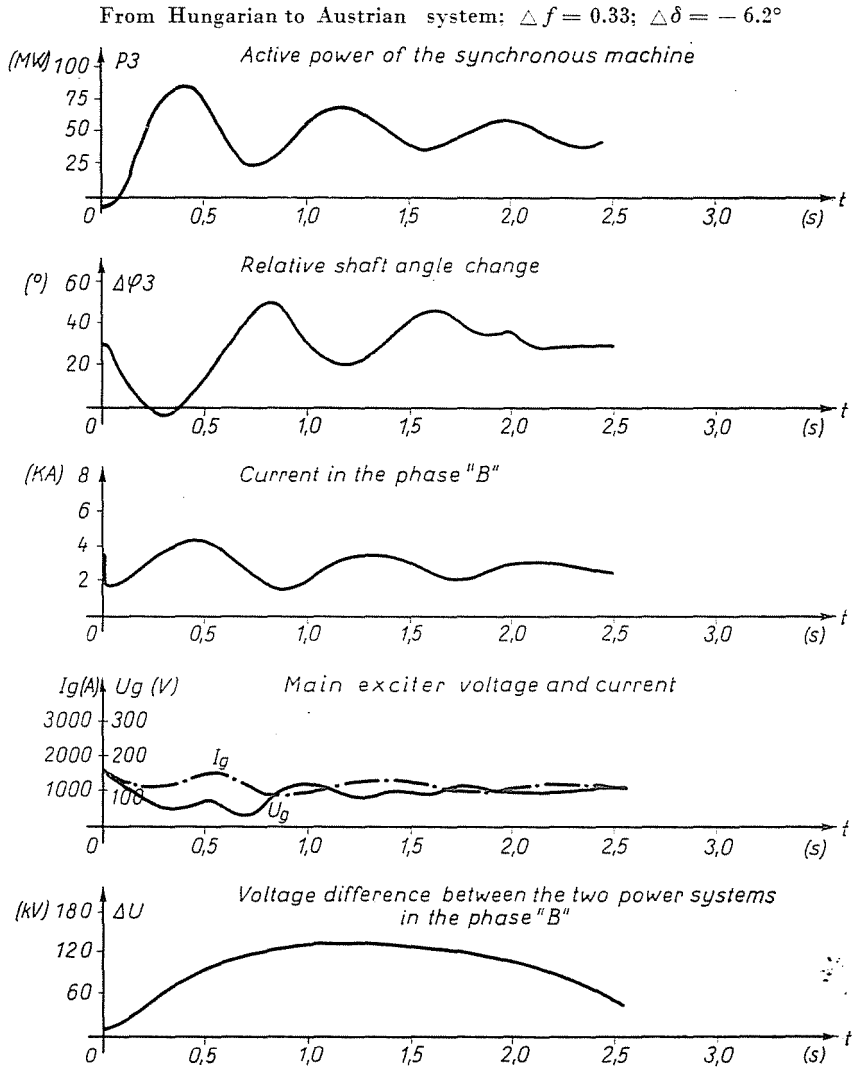

MEASURED VALUES

Diagram 2

analyses showed that a shaft-coupling torque switch occurred at the present allowed maximum frequency difference $\Delta f = 0.7$ Hz, when the terminal voltage of the machine (transformer) was forward by 13° or backward by 16°

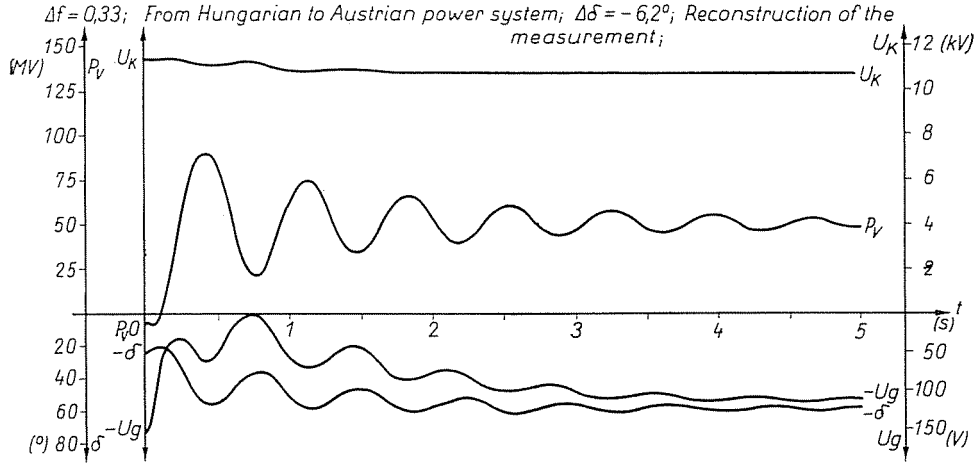

ANALOG SIMULATION

Diagram 3

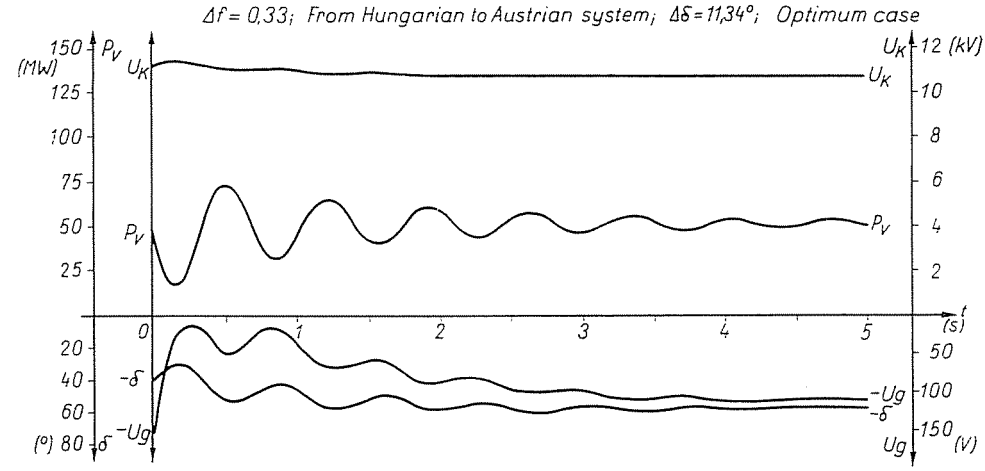

ANALOG SIMULATION

Diagram 4

in average, related to the optimal switching angle. At the same time the maximum of the first positive electric power peak following the switching was 3.2 times the nominal value.

2.4. *The influence of the reactive power before switching*

The effect of the value of the reactive power given by the generator in the steady-state preceding the switching is not quite definite. For a higher reactive power the change of the moment occurs sooner, on the other hand, the stability relations are better. (The amplitude of the first positive peak is less and the damping of the oscillation is better.) None of these opposing

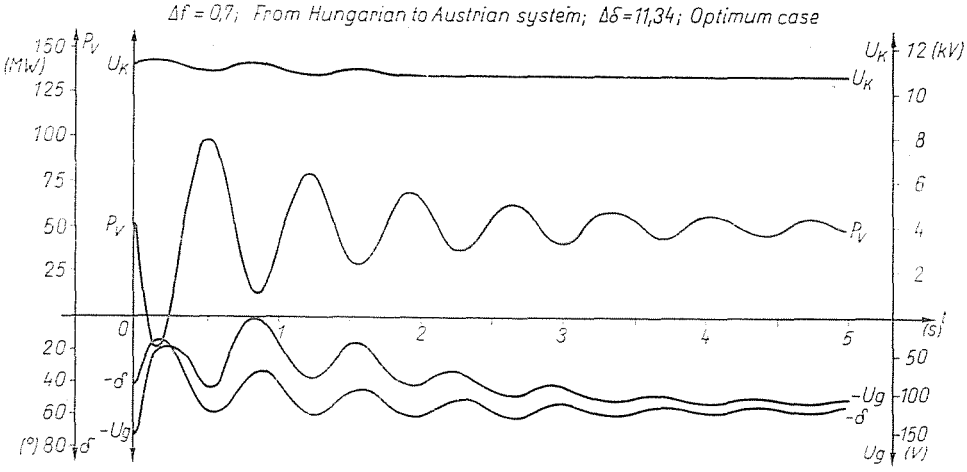

ANALOG SIMULATION

Diagram 5

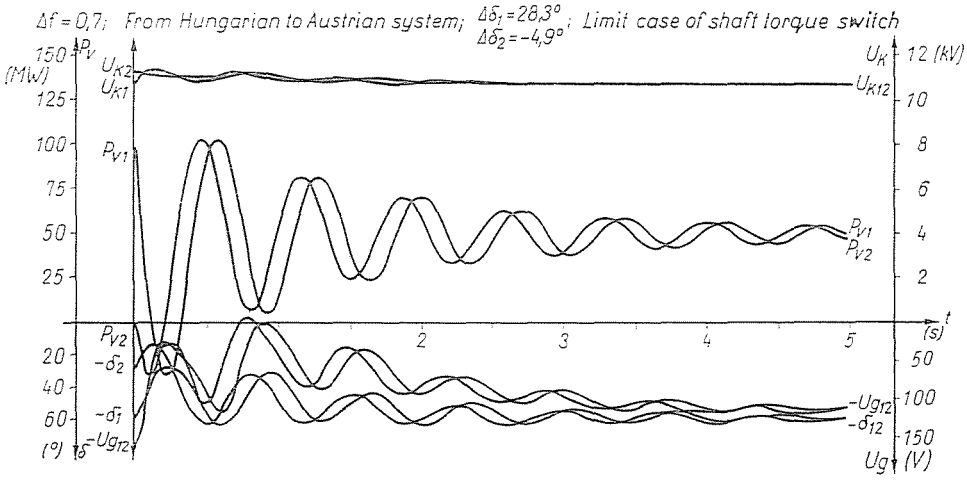

ANALOG SIMULATION

Diagram 6

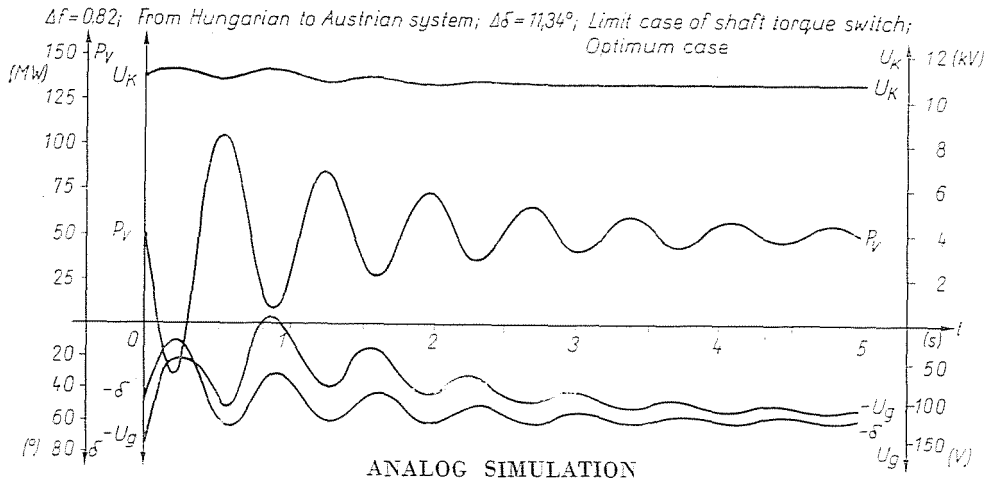

ANALOG SIMULATION

Diagram 7

From Austrian to Hungarian system; $\triangle f = 0.35$; $\triangle \delta = -0.2°$

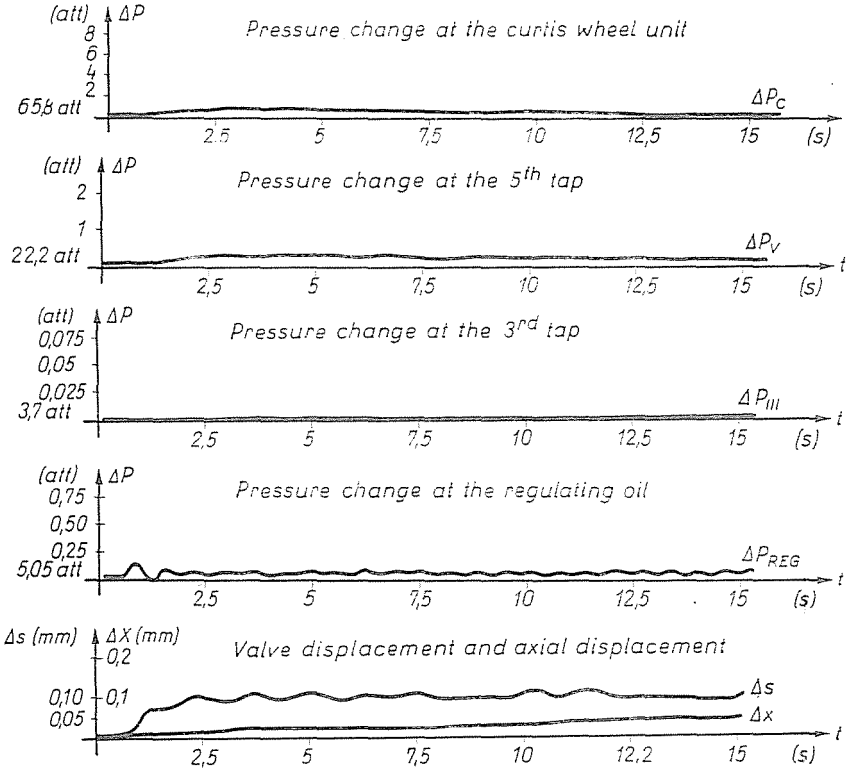

MEASURED VALUES

Diagram 8

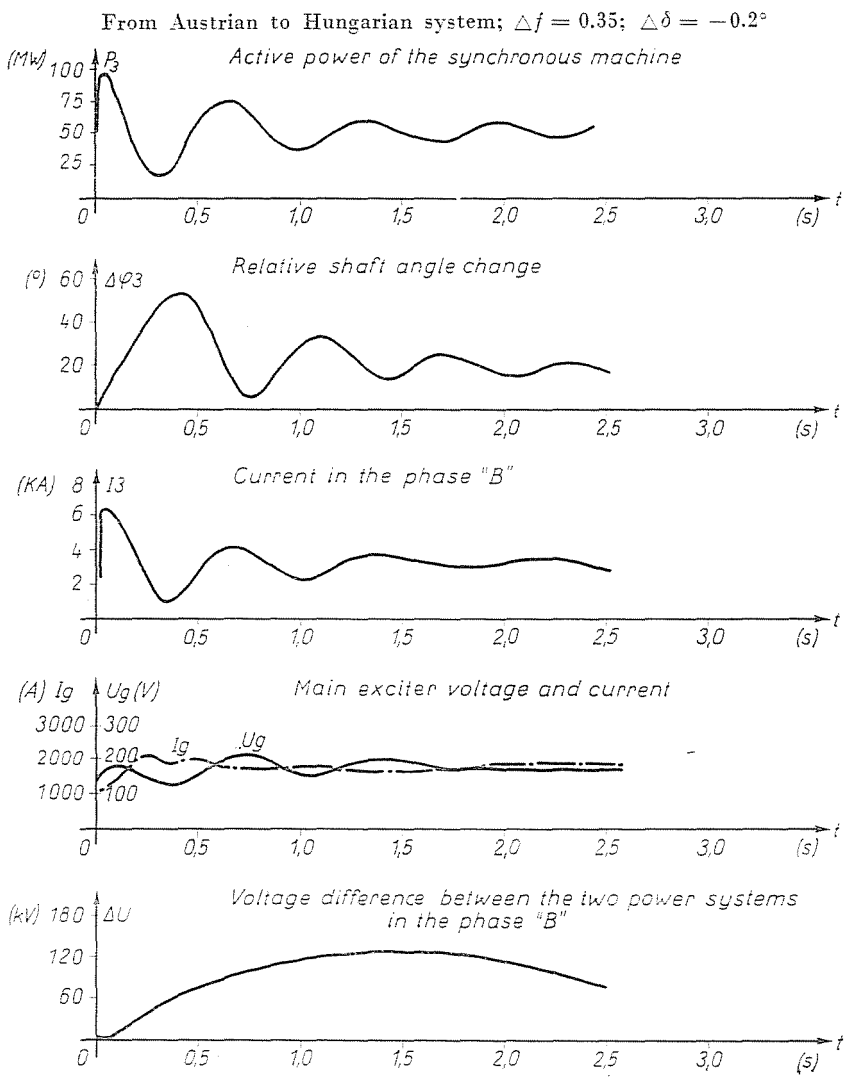

MEASURED VALUES

Diagram 9

effects are as important, as the influence of e.g. $\Delta\delta$, which can be numerically illustrated by the following:

a) In the case of positive Δf, if $\Delta f = 0.35$ Hz at optimal switching angle the first negative power peak for 40 MVAr reactive power is by about 7 per cent higher than for 10 MVAr: the same difference for $\Delta f = 0.7$ is about 20 per cent. The first positive power peak and the damping are, however, by 6 per cent better for high than for low reactive power.

The $\Delta\delta$ interval of the switching without shaft-coupling moment switch is 20 per cent wider for low than for high reactive power.

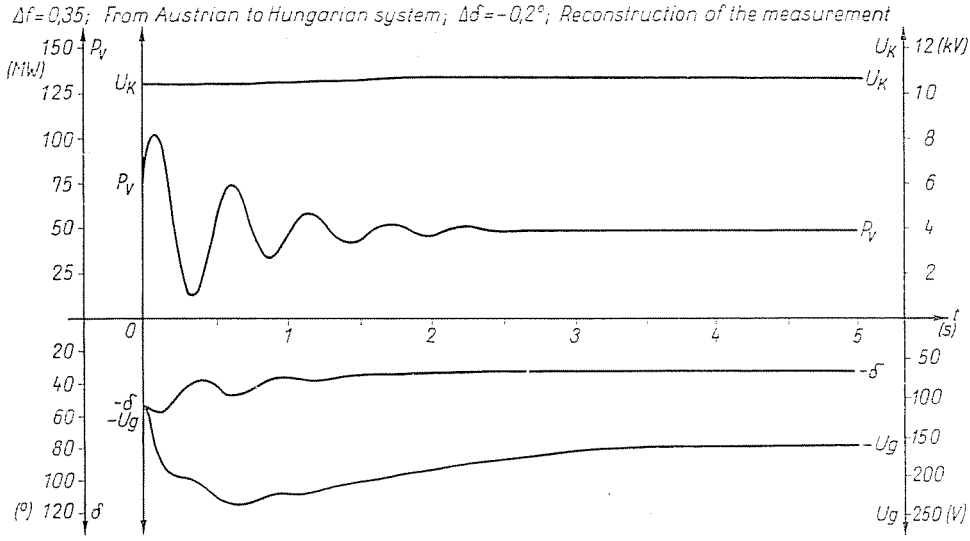

ANALOG SIMULATION

Diagram 10

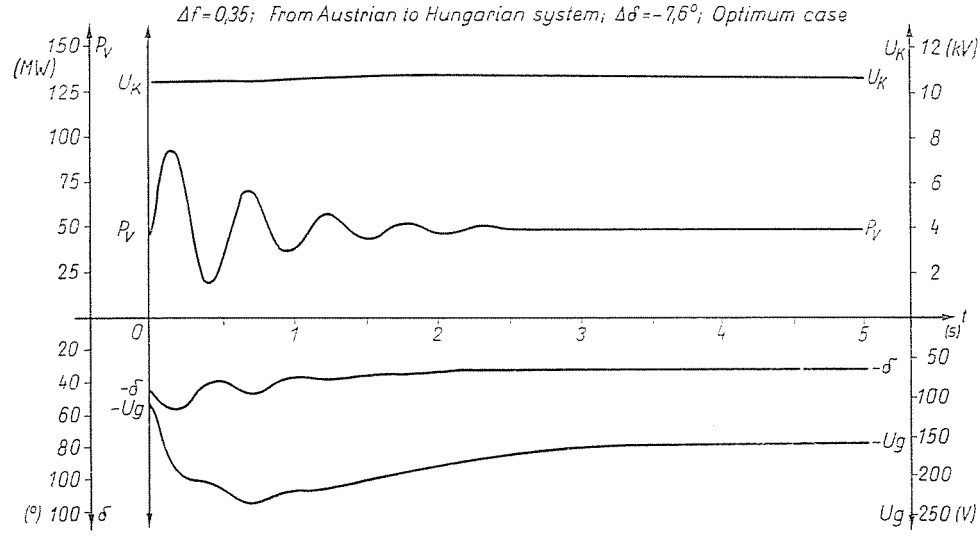

Diagram 11

ANALOG SIMULATION

b) In the case of negative Δf the influence of the reactive load is less than in the case a), so it is practically negligible.

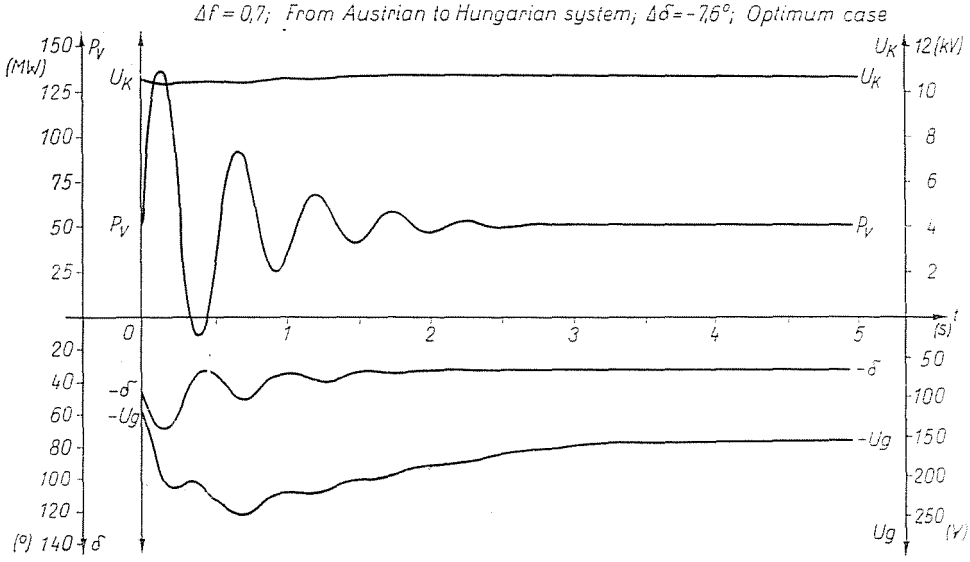

ANALOG SIMULATION

Diagram 12

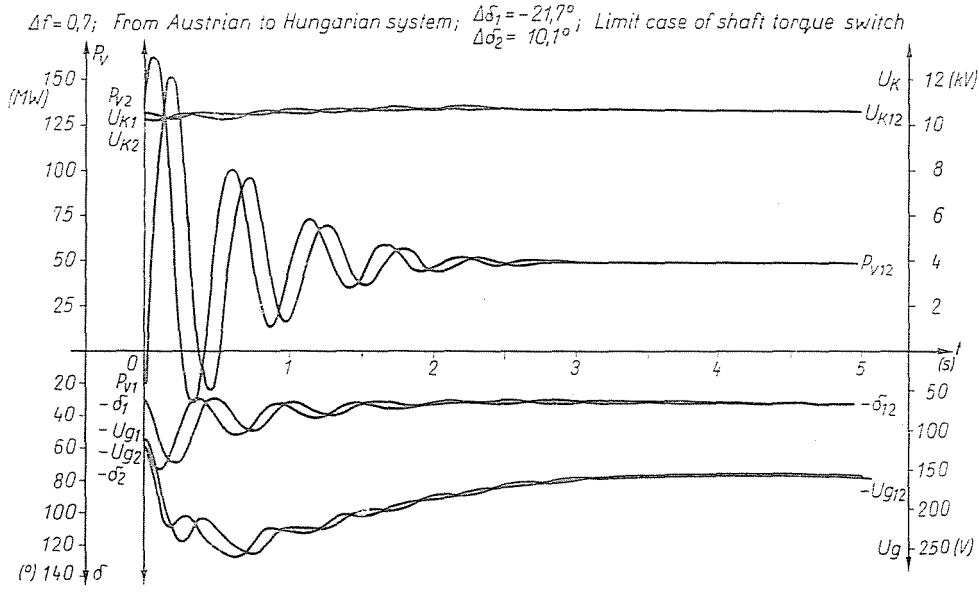

ANALOG SIMULATION

Diagram 13

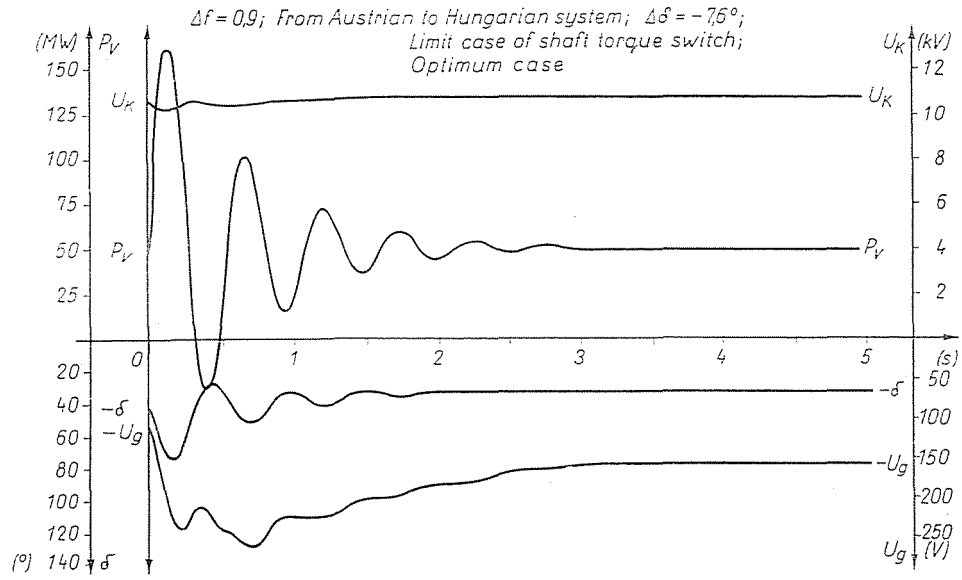

ANALOG SIMULATION

Diagram 14

2.5. The influence of the quick voltage regulator

Both in the course of the field test measurements and in the analog simulations, for the investigation of the influence of the quick voltage regulator, in part of the analysed cases the excitation voltage was kept constant, in the other cases the regulator worked. Comparing the results it could be stated that the influence of the automatic voltage regulation was favourable from the point of view of mechanical stresses but this effect was not important.

Acknowledgement

The authors wish to thank Lajos Petri, engineer in the Factory Láng, for the useful advices and informations which was provided an important aid in successfully carrying out the analysis.

APPENDIX 1

Mathematical Model of 50 MW Condensation Type Steam Turbine — Control Block System, for the Investigation of Pseudo-synchronous Switchings

The block diagram of the system is shown in Fig. 1.1. The I. is the controller, II. is the controlled object. The variables $x_1, x_2, x_3 \ldots$ are the deviations of the system signals from working point values in relative units. g_1, g_2, g_3, g_4

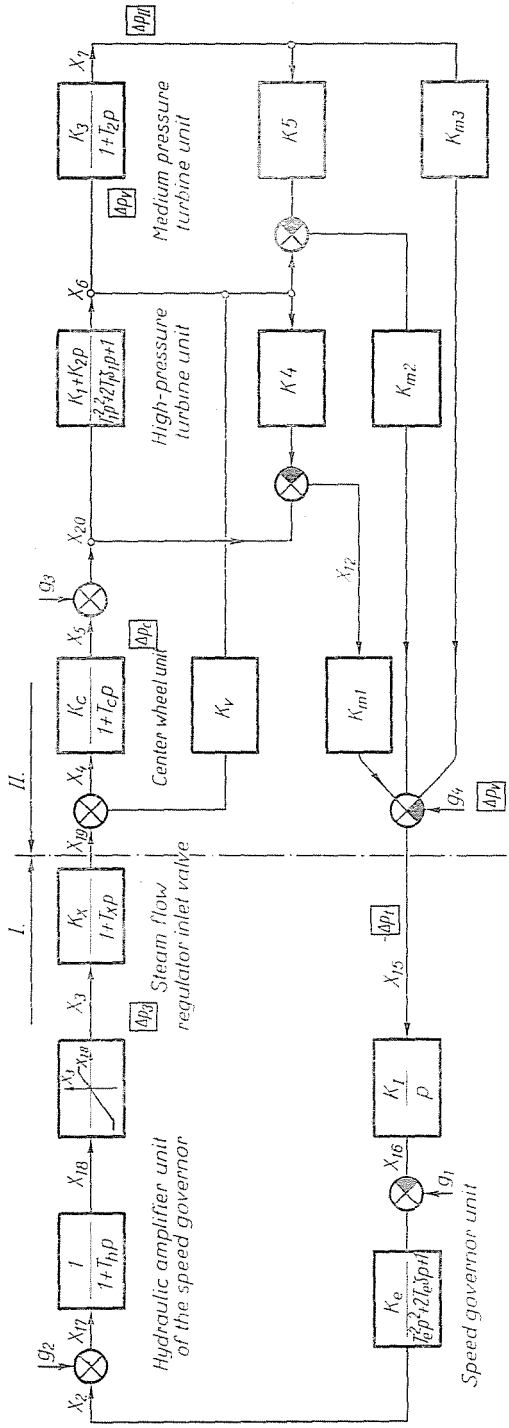
Hydraulic amplifier unit of the speed governor
Steam flow regulator inlet valve
Center wheel unit
High-pressure turbine unit
Medium pressure turbine unit
Speed governor unit
I.
II.

Fig. 1.1

are the command signal, the modifying signal of the Local Power-Frequency Regulator, the steam and generator side disturbances, resp. (also in relative units). The elements in the block diagram will be discussed individually.

1.1. Speed governor unit (weights, spring, piston, etc.) transfer function

$$\frac{x_2}{x_1} = \frac{K_e}{T_e^2 p^2 + 2T_e \xi_e p + 1} \tag{1.1}$$

where

$$x_2 = \frac{\Delta p_s}{p_{sn}}$$

$\Delta p_s = p_s - p_{sm}$

p_s — controlling pressure

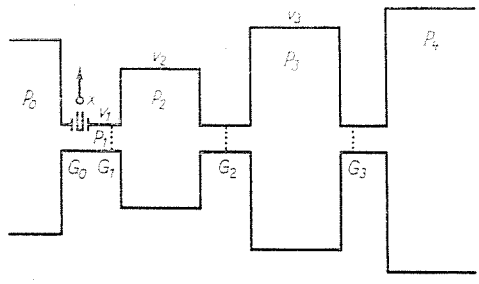

Fig. 1.2

p_{sm} — working point value of the controlling pressure

$$p = \frac{d}{dt}$$

p_{sn} — nominal value of the same pressure

T_e — time constant

ξ_e — damping coefficient

K_e — transfer coefficient for the given working point

$$K_e = -\frac{n_n}{p_{sn}} \cdot \frac{\partial p_s}{\partial n} \tag{1.2}$$

n_n — nominal speed of rotation.

1.2. Hydraulic amplifier unit of the speed governor

The transfer function of this unit is

$$\frac{x_{18}}{x_{17}} = \frac{1}{1 + T_h p} \tag{1.3}$$

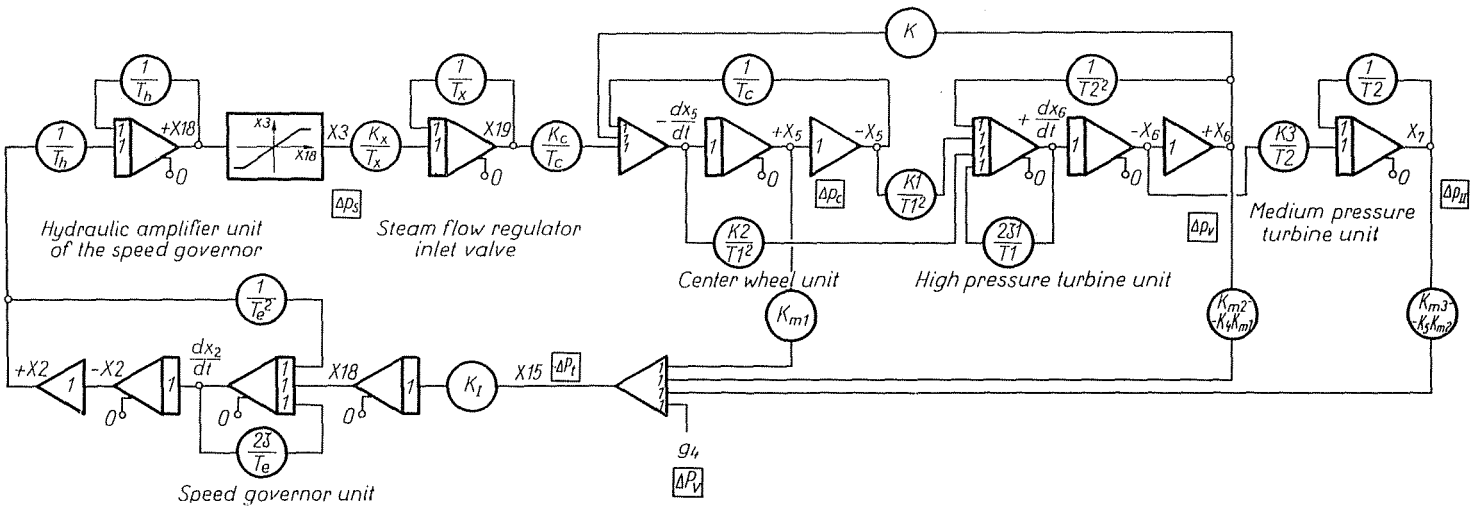
Hydraulic amplifier unit of the speed governor
Steam flow regulator inlet valve
Center wheel unit
High pressure turbine unit
Medium pressure turbine unit
Speed governor unit

Fig. 1.3

1.3. Steam flow regulator inlet valve

The transfer function of the valve is

$$\frac{x_{19}}{x_3} = \frac{K_x}{1+T_x p} \tag{1.4}$$

where:

$$x_{19} = \frac{\Delta x}{x_\Sigma}$$

$$\Delta x = x - x_m$$

and the meaning of the symbols used:

x — displacement of the valve
x_m — displacement of the valve in the working point position
x_Σ — the whole displacement
T_x — time constant.

1.4. The turbine as the controlled object

The turbine can be analysed on the basis of the principal scheme shown in Fig. 1.2.

The steam flows (G_1, G_2, G_3) through the units of the turbine, depend on the pressures before and after the units (p_1, p_2, p_3, p_4) and on the speed of rotation.

Because of the small variation, the dependence on the speed of rotation may be neglected.

Thus:

$$G_1 = f_1(p_1, p_2) \tag{1.5}$$

$$G_2 = f_2(p_2, p_3) \tag{1.6}$$

$$G_3 = f_3(p_3, p_4)\,. \tag{1.7}$$

The steam flow through the control valve is

$$G_0 = f_0(p_0, p_1, x) \tag{1.8}$$

(p_0 is the steam pressure before the valve).

For small variations:

$$\Delta G_0 = \frac{\partial f_0}{\partial p_0}\Delta p_0 + \frac{\partial f_0}{\partial p_1}\Delta p_1 + \frac{\partial f_0}{\partial x}\Delta x \tag{1.9}$$

$$\Delta G_1 = \frac{\partial f_1}{\partial p_1}\Delta p_1 + \frac{\partial f_1}{\partial p_2}\Delta p_2 \tag{1.10}$$

$$\Delta G_2 = \frac{\partial f_2}{\partial p_2}\Delta p_2 + \frac{\partial f_2}{\partial p_3}\Delta p_3 \tag{1.11}$$

$$\Delta G_3 = \frac{\partial f_3}{\partial p_3}\Delta p_3 + \frac{\partial f_3}{\partial p_4}\Delta p_4 \tag{1.12}$$

where Δp_0, Δp_1, Δp_2, Δp_3 and Δp_4 are the pressure variation.

The variations on the steam side are taken into consideration separately, so here the value $\Delta p_0 = 0$ may be considered.

Also,

$$\Delta p_4 = 0\,.$$

For the steam flows the following equation is known:

$$(\Delta G_0 - \Delta G_1)dt = V_1 d\gamma_1 \tag{1.13}$$

where

V_1 — is the volume

γ_1 — is the specific gravity.

The change of conditions of the steam may be considered polytropical. Thus

$$p_1\gamma_1^{-n} = p_{1m}\gamma_{1m}^{-n} = \text{const.}$$

(It is known from the literature, that $n \approx 1$.)

$$d\gamma_1 = c_1 dp_1$$
$$(c_1 = \text{constans.})$$

On the basis of the above:

$$a_0\Delta p_1 + a_1\frac{d\Delta p_1}{dt} = e_0\Delta x + b_0\Delta p_2 \tag{1.14}$$

(the coefficients a_0, a_1, e_0, b_0 can easily be expressed analytically).

Furthermore:

$$/\Delta G_1 - \Delta G_2/dt = V_2 d\gamma_2 \tag{1.15}$$

and

$$/\Delta G_2 - \Delta G_3/dt = V_3 d\gamma_3. \tag{1.16}$$

Similarly:

$$a_2\Delta p_2 + a_3\frac{d\Delta p_2}{dt} = b_1\Delta p_1 + b_2\Delta p_3 \tag{1.17}$$

and

$$a_4 \Delta p_3 + a_5 \frac{d\Delta p_3}{dt} = b_3 \Delta p_2 \,. \tag{1.18}$$

From these expressions

$$a_6 \Delta p_2 + a_7 \frac{d\Delta p_2}{dt} + a_8 \frac{d^2 \Delta p_2}{dt^2} = b_4 \Delta p_1 + b_5 \frac{d\Delta p_1}{dt} \,. \tag{1.19}$$

On the block diagram in Fig. 1.1, the relations of the pressures obtained in the above expressions are shown.

The variation of the pressure at the Curtis wheel follows the motion of the valve, practically without any time delay. Coefficient a_1 is very small and comparing with the effect of the valve movement, Δx, the effect of the variation of the pressure, Δp_2, is also small ($b_0 \approx 0$).

Notations used in Fig. 1.1 are:

$$\Delta p_1 = x_5$$
$$\Delta p_2 = x_6$$
$$\Delta p_3 = x_7 \,.$$

Disturbances from the steam side may be taken into consideration as the variation of the pressure before the high-pressure turbine unit.

$$x_{20} = x_5 + g_3$$

where g_3 — represents the disturbances.

From the above expressions the following transfer functions are obtained:

$$\frac{x_5}{x_4} = \frac{K_c}{1 + T_c p} \tag{1.20}$$

where

$$x_4 = x_{19} + K_v x_6$$

$$\frac{x_6}{x_{20}} = \frac{K_1 + K_2 p}{T_1^2 p^2 + 2T_1 \zeta_1 p + 1} \tag{1.21}$$

$$\frac{x_7}{x_6} = \frac{K_3}{1 + T_2 p} \,. \tag{1.22}$$

(The notations of the coefficients are straightforward.)

1.5. Torque Equations of the Turbine

The torques generated by the turbine units are considered also as non-linear functions of the pressures before and after the units:

$$M_1 = M_1(p_1, p_2) \tag{1.23}$$

$$M_2 = M_2(p_2, p_3) \tag{1.24}$$

$$M_3 = M_3(p_3) \tag{1.25}$$

For small variations:

$$\Delta M_1 = \frac{\partial M_1}{\partial p_1}\Delta p_1 + \frac{\partial M_1}{\partial p_2}\Delta p_2 = K_{m1}(\Delta p_1 - K_4 \Delta p_2) \tag{1.26}$$

$$\Delta M_2 = \frac{\partial M_2}{\partial p_2}\Delta p_2 + \frac{\partial M_2}{\partial p_3}\Delta p_3 = K_{m2}(\Delta p_2 - K_5 \Delta p_3) \tag{1.27}$$

$$\Delta M_3 = \frac{\partial M_3}{\partial p_3}\Delta p_3 = K_{m3}\Delta p_3 . \tag{1.28}$$

The variation of the turbine torque is:

$$\Delta M_T = \Delta M_1 + \Delta M_2 + \Delta M_3 . \tag{1.29}$$

Accordingly, the variation of the generated power is

$$\Delta P_t = \omega \cdot \Delta M_T . \tag{1.30}$$

The analog computer block scheme for the steam turbine speed governor system simulation is shown in Fig. 1.3.

APPENDIX 2

The Analog Computer Model of the Synchronous Generator and Voltage Regulation System

2.1. The Model of the Voltage Regulator AVR

a) The regulator — as its basic principle — is an apparatus of magnetic amplifier and of semiconductor system provided by current and reactive power limits. (In our analysis these latter were neglected, taking into account that according to the field test measurements they operated in no case.) The scheme of the apparatus is shown in Fig. 2.1.

The main elements of the system:

1. Comparator
2. Preamplifier
3. Terminal amplifier

The block scheme is shown in Fig. 2.2.

b) Exciter

The output voltage of the terminal amplifier acts on the control winding of the main exciter. The other excitation winding is of shunt connection, and it is set in so that the shunt line has to approach the air gap line. In steady state the main exciter is excited by the shunt winding, the control winding produces only the relatively little excitation value, necessary for compensating the difference between the shunt-line and the characteristic. In simulating the dynamic performance of the main exciter, the scheme in Fig. 2.3. is applied.

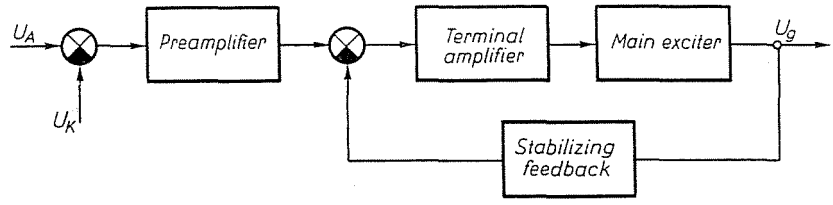

Fig. 2.1

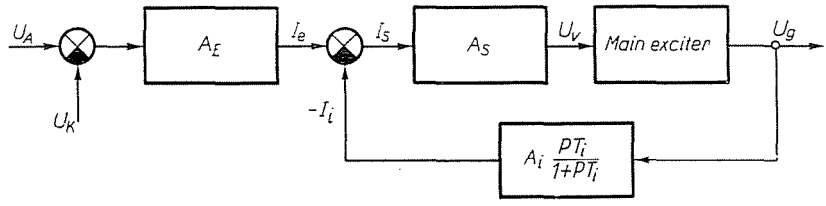

Fig. 2.2

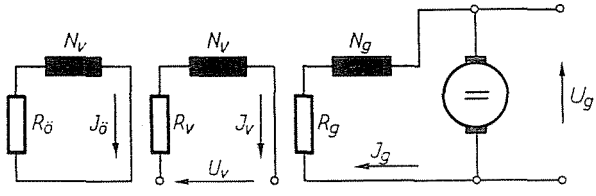

Fig. 2.3

The effect of the eddy currents arising at the change of the main flux is considered by the short circuited excitation winding of number of turns N_v and of fictitious resistance $R_{\ddot{o}}$. The internal resistance of the terminal amplifier is the resistance R_b. Based on Fig. 2.3, the following equations can be written:

$$U_v = R_v I_v + N_v \frac{d\Phi}{dt} \tag{2.1}$$

$$0 = R_{\ddot{o}} I_{\ddot{o}} + N_v \frac{d\Phi}{dt} \tag{2.2}$$

$$U_g = R_g I_g + N_g \frac{d\Phi}{dt} \tag{2.3}$$

$$U_g = C\Phi \tag{2.4}$$

$$N_g I'_g = I_v N_v + I_g N_g + I_{\bar{0}} N_v \tag{2.5}$$

$$I'_g = f(U_g)$$

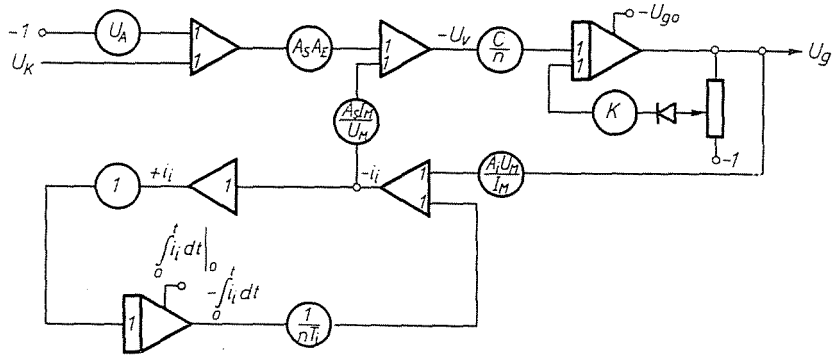

Fig. 2.4

(on account of the saturation given as characteristic).

From the solution of the equations the following relations are obtained

$$\frac{dU_g}{dt} = bU_g - af(U_g) + cU_v \tag{2.6}$$

where

$$B = \frac{(R_{\bar{0}} + R_v) N_v^2}{N_g C R_{\bar{0}} R_v} + \frac{N_g}{C R_g}; \quad a = \frac{1}{B}; \quad b = \frac{1}{R_g B}; \quad c = \frac{N_v}{N_g R_v B}. \tag{2.7}$$

The main exciter behaves as an integrating element in the non-saturated domain and as a one-storage proportional element in the saturated one. The analog computer scheme based on the diagram of Fig. 2.2 and on Eqs 2.1 through 2.7 is given in Fig. 2.4.

2.2. The Model of the Synchronous Generator

In the analog computer model of the 50 MW synchronous generator the following suppositions were made (the legend is given in Appendix 4).

a) The basis of the model is the system of the Park equations of the synchronous generator, as follows:

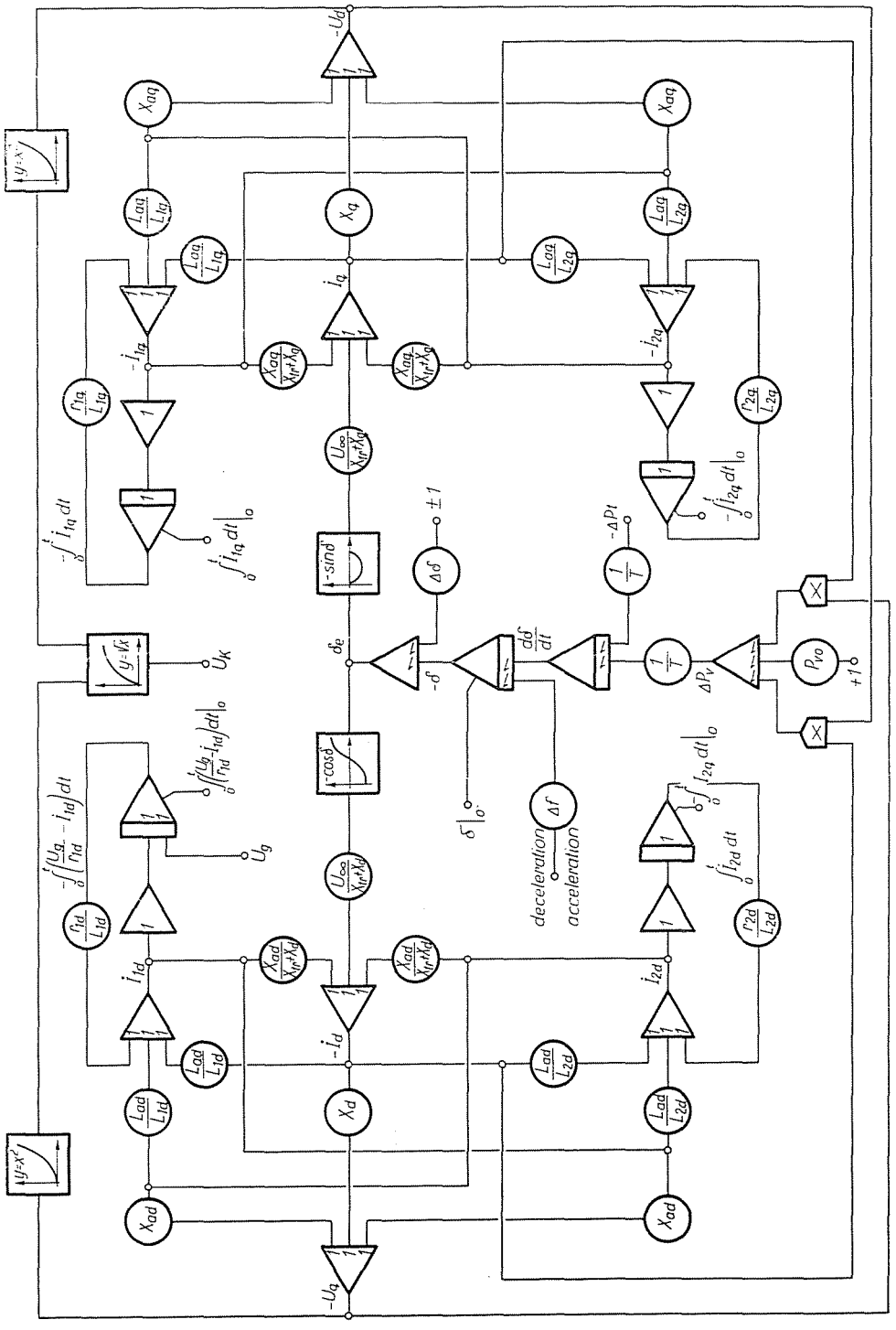

Fig. 2.5

1. Flux equations

$$\psi_d = L_{ad}(i_{1d} + i_{2d}) - L_d i_d \tag{2.8}$$

$$\psi_q = L_{aq}(i_{1q} + i_{2q}) - L_q i_q \tag{2.9}$$

$$\psi_{1d} = L_{1d} i_{1d} + L_{ad}(i_{2d} - i_d) \tag{2.10}$$

$$\psi_{2d} = L_{2d} i_{2d} + L_{ad}(i_{1d} - i_d) \tag{2.11}$$

$$\psi_{1q} = L_{1q} i_{1q} + L_{aq}(i_{2q} - i_q) \tag{2.12}$$

$$\psi_{2q} = L_{2q} i_{2q} + L_{aq}(i_{1q} - i_q)\,. \tag{2.13}$$

According to the general practice it is supposed that all of the direct-axis mutual inductivities are L_{ad} and all of the quadrature-axis ones are L_{aq}.

2. Voltage equations

$$U_d = \frac{d\psi_d}{dt} - \omega \cdot \psi_q - r i_d \tag{2.14}$$

$$U_q = \frac{d\psi_q}{dt} + \omega \cdot \psi_d - r i_q \tag{2.15}$$

$$U_g = \frac{d\psi_{1d}}{dt} + r_{1d}\, i_{1d} \tag{2.16}$$

$$0 = \frac{d\psi_{2d}}{dt} + r_{2d}\, i_{2d} \tag{2.17}$$

$$0 = \frac{d\psi_{1q}}{dt} + r_{1q}\, i_{1q} \tag{2.18}$$

$$0 = \frac{d\psi_{2q}}{dt} + r_{2q}\, i_{2q}\,. \tag{2.19}$$

3. Electric moment equation

$$\frac{P_r}{\omega} = \psi_d\, i_q - \psi_q\, i_d\,. \tag{2.20}$$

b) Since among the given data there were no quadrature-axis parameters, followings were supposed (partly according to literature data but mainly according to the results of the field test measurements):

$$X_q = X_d$$
$$X'_q = 1.5\, X'_d$$
$$X''_q = X''_d$$

$$T'_{q0} = \frac{1}{9} T'_{d0}$$

$$T''_{q0} = T''_{d0}.$$

An additional supposition based on the maximum incidence with the measurements is:

$$X_s = 0.104 \text{ p.u.}$$

c) Concerning the reactances the saturated values belonging to the nominal load point were taken into consideration. In course of the simulation, the effect of the reactance change caused by the change of saturation was neglected, since its influence on the transient phenomena was unimportant for a small change of the terminal voltage.

d) In the voltage equations of the armature, the effect of the D. C. armature current component decaying in a period less than 0.1 sec according to the measurements was not simulated. Namely, in these equations the terms $d\psi/dt$ are neglected beside the $\omega\psi$ terms in correspondence with the literature.

e) The resistances of the armature and of the circuit linked galvanically with it, are neglected, because their sum is less than 10 per cent of the total impedance and so the error in the results does not exceed 1 per cent.

f) The change of the reactance caused by the "frequency step" is neglected as well, since its maximum value does not exceed 1.4 per cent.

Consequently, the system of equations of the synchronous machine applied directly for the analog simulation is the following:

$$U_d = -X_{aq} i_{1q} - X_{aq} i_{2q} + X_q i_q \tag{2.21}$$

$$U_q = X_{ad} i_{1d} + X_{ad} i_{2d} - X_d i_d \tag{2.22}$$

$$i_d = \frac{X_{ad}}{X_{tr}+X_d}(i_{1d} + i_{2d}) - \frac{1}{X_{tr}+X_d} U_\infty \cos\delta \tag{2.23}$$

$$i_q = \frac{X_{aq}}{X_{tr}+X_q}(i_{1q} + i_{2q}) + \frac{1}{X_{tr}+X_q} U_\infty \sin\delta \tag{2.24}$$

$$i_{1d} = \frac{1}{L_{1d}} \psi_{1d0} + L_{ad}(i_d - i_{2d}) + \int_0^t (U_g - r_{1d} i_{1d})\, dt \tag{2.25}$$

$$i_{2d} = \frac{1}{L_{2d}} \psi_{2d0} + L_{ad}(i_d - i_{1d}) - \int_0^t r_{2d}\, i_{2d}\, dt \tag{2.26}$$

$$i_{1q} = \frac{1}{L_{1q}} \psi_{1q0} + L_{aq}(i_q - i_{2q}) - \int_0^t i_{1q} r_{1q}\, dt \tag{2.27}$$

$$i_{2q} = \frac{1}{L_{2q}} \psi_{2q0} + L_{aq}(i_q - i_{1q}) - \int_0^t i_{2q} r_{2q}\, dt . \tag{2.28}$$

In the analog computer program the

$$\frac{\psi_{1d0}}{L_{1d}}, \frac{\psi_{2d0}}{L_{2d}}, \frac{\psi_{1q0}}{L_{1q}}, \frac{\psi_{2q0}}{L_{2q}}$$

values are the starting conditions of the integrators.

$$U_k = \sqrt{U_d^2 + U_q^2} \tag{2.29}$$

$$\Delta P_v = U_d i_d + U_q i_q - P_{v0} \tag{2.30}$$

$$T \frac{d^2 \delta}{dt^2} = \Delta P_t - \Delta P_v . \tag{2.31}$$

The block diagram of the analog computer program corresponding to the equations above are showed on Fig. 2.5.

APPENDIX 3

The Method of Simulation of the Measured Cases

The series of calculations on the analog computer were always based on the correct simulation of the cases of the field test measurements that is to say computer simulation of the time functions of all the important parameters obtained in the measurement were carried out. This was followed by changing the parameters (primarily the frequency step and the angle difference to the synchronous position at the moment of switching) which were not or only slightly possible to change on the field test measurement (see Appendix 2). Concerning the parameter $\Delta\delta$, it should be mentioned in physical sense that it is the angle between the infinite bus-bar voltages before and after the switching at the moment of switching, according to the principle of the simulation (see the analog computer block diagram).

The simulation of the cases of the measurement was carried out in the following steps:

a) In the studied case the representation of the steady-state preceding the switching by setting in the potentiometer values calculated preliminarily.

b) Thereafter, to simulate the transients after the pseudo-synchronous switching, the potentiometer s were set again, the values of which corresponded to the value of the transfer impedance between the infinite bus-bar and the generator terminals. Then the power step occurring at synchronous angle position could be determined by the analog computer.

c) Thereafter in "problem check" position the setting in of the potentiometers belonging to $\Delta\delta$ was changed until the electric power step observed achieved the value obtained at the field test measurement.

d) At last, by setting in the potentiometer marked Δf, according to the frequency step corresponding to the actual measured case and putting the computer in "compute" position, the change in course of the switching of the most important parameters were registered. Since the quadrature-axis time constant (T'_{q0}) was a free parameter — neither calculated nor directly measured value was available for it — it was determined by the reproduction of the swing damping occurred in the field test measurement. This was at $T'_{q0} = \frac{1}{9} T'_{d0}$ which is in quite good agreement with the data given in the literature.

It is to be mentioned that in all of the cases the terminal voltage of the synchronous generator was supposed to be of nominal value (10.5 kV), since in this way the pretransient state could be calculated simply and exactly from the real and reactive powers measured on the terminals.

There was a good agreement between the measured and calculated curves of the excitation voltage (the swings of second harmonic were neglected in the measurements in some particular cases that had little influence on the basic phenomenon).

APPENDIX 4

Legend

Quantities of the Synchronous Generator

Voltages

U_d — direct-axis component of the terminal voltage
U_q — quadrature-axis component of the terminal voltage
U_e — instantaneous value of the excitation voltage
U_∞ — voltage of the infinite bus-bar
U_k — instantaneous value of the terminal voltage $U_k = \sqrt{U_d^2 + U_q^2}$

Currents

i_d — direct-axis component of the armature current
i_q — quadrature-axis component of the armature current
i_{1d} — excitation current
i_{1q} — quadrature-axis fictitious excitation current
i_{2d} — direct-axis amortisseur current
i_{2q} — quadrature-axis amortisseur current

Fluxes

ψ_d — direct-axis component of the stator flux linkage
ψ_q — quadrature-axis component of the stator flux linkage
ψ_{1d} — field flux linkage
ψ_{1q} — quadrature-axis fictitious field flux linkage
ψ_{2d} — direct axis amortisseur flux linkage
ψ_{2q} — quadrature-axis amortisseur flux linkage

Inductances

L_d — direct-axis stator self-inductance
L_q — quadrature-axis stator self-inductance
L_{1d} — excitation circuit self-inductance
L_{1q} — quadrature-axis fictitious excitation circuit self-inductance
L_{2d} — direct-axis amortisseur self-inductance
L_{2q} — quadrature-axis amortisseur self-inductance
L_{ad} — direct-axis mutual inductance
L_{aq} — quadrature-axis mutual inductance

Impedances

X_d — direct-axis synchronous reactance
X_q — quadrature-axis synchronous reactance
X_{ad} — direct-axis mutual reactance
X_{aq} — quadrature-axis mutual reactance
X_{tr} — transfer reactance
r_{1d} — excitation circuit resistance
r_{1q} — quadrature-axis fictitous circuit resistance
r_{2d} — direct-axis amortisseur resistance
r_{2q} — quadrature-axis amortisseur resistance
X'_d — direct-axis transient resistance
X'_q — quadrature-axis transient reactance

Other quantities

$\Delta f = f_{\text{Austria}} - f_{\text{Hungary}}$ = frequency difference between the Hungarian and the Austrian system (frequency step)
ΔP_v — the increment of power supplied by the synchronous machine into the network
ΔP_t — turbine power increment
P_{v0} — pretransient value of the electric power
T — angular momentum of the turbine-generator group
δ — angle difference between the voltage vector of the infinite bus-bar and the quadrature-axis
T'_{d0} — direct-axis no-load time constant
T'_{q0} — quadrature-axis no-load time constant
T'_{d0} — direct-axis no-load time constant
T'_{q0} — quadrature-axis no-load time constant

Quantities concerning the voltage regulator

U_v — output voltage of the AVR
U_g — output voltage of the main exciter
I_v — output current of the AVR
I_g — exciting current of shunt winding of the main exciter
I'_g — fictitious exciting current
$I_{\bar{o}}$ — fictitious eddy current
Φ — flux of the main exciter
N_g — number of turns of the shunt winding of the main exciter
N_v — number of turns of the external winding of the main exciter
R_b — the output resistance of the AVR

APPENDIX 5

Data used in the analysis

Oroszlány Power Plant Block III.
Electric parameters of the synchronous machine:

U_n = 10.5 kV
S_n = 67 MVA
cos fi = 0.75
X_d = 180%
X'_d = 17%
X''_d = 11%
T'_{do} = 7.6 s
T''_{do} = 0.05s

Turbo-generator unit, nonelectric parameters:
$GD^2_{turbine}$ = 14.9 tm²
$GD^2_{generator}$ = 8.85 tm²

Summary

In consequence of the special characteristics of the Hungarian and Austrian power systems their mutual energy transports — regulated by appropriate import-export contract — must be realized without the two systems being interconnected.

Following this strict condition it occurs rather frequently that some of the — fully loaded — generating units of the Thermal Power Plant in Oroszlány have to be switched over from the Hungarian to the Austrian power system the frequencies of which may have deviations in the order of 0.1—0.7 Hz from each other.

In the following paper a brief description is given on the results and theoretical inferences of the field tests and analog simulations carried out in order to study the transient phenomena of the generating units following this so called "pseudo-synchronous" switching process.

Prof. Dr. Ottó P. Geszti
Dr. László Zoltán Rácz
Lajos Kiss
István Horváth
Dr. János Somló

1502 Budapest, P. O. B. 91. Hungary